UC Berkeley
UC Berkeley Previously Published Works

Title

An array of Zymoseptoria tritici effectors suppress plant immune responses.

Permalink

https://escholarship.org/uc/item/9kr339h7

Journal

Molecular Plant Pathology, 25(10)

Authors

Thynne, Elisha

Ali, Haider

Seong, Kyungyong

et al.

Publication Date

2024-10-01

DOI

10.1111/mpp.13500

Peer reviewed

ORIGINAL ARTICLE

An array of *Zymoseptoria tritici* effectors suppress plant immune responses

Elisha Thynne[1,2] | Haider Ali[3] | Kyungyong Seong[4] | Mohammad Abukhalaf[5] | Marco A. Guerreiro[1,2] | Victor M. Flores-Nunez[1,2] | Rune Hansen[1,2] | Ana Bergues[1,2] | Maja J. Salman[1] | Jason J. Rudd[6] | Kostya Kanyuka[7] | Andreas Tholey[4] | Ksenia V. Krasileva[5] | Graeme J. Kettles[3] | Eva H. Stukenbrock[1,2]

[1]Botanical Institute, Christian-Albrechts University, Kiel, Germany

[2]Max Planck Institute for Molecular Biology, Plön, Germany

[3]School of Biosciences, University of Birmingham, Birmingham, UK

[4]Department of Plant and Molecular Biology, University of California, Berkeley, California, USA

[5]Institute for Experimental Medicine, Christian-Albrechts University (UK-SH Campus), Kiel, Germany

[6]Department of Plant Biology and Crop Science, Rothamsted Research, Harpenden, UK

[7]National Institute of Agricultural Botany (NIAB), Cambridge, UK

Correspondence
Elisha Thynne, Botanical Institute, Christian-Albrechts University, Kiel 24118, Germany.
Email: ethynne@bot.uni-kiel.de

Abstract

Zymoseptoria tritici is the most economically significant fungal pathogen of wheat in Europe. However, despite the importance of this pathogen, the molecular interactions between pathogen and host during infection are not well understood. Herein, we describe the use of two libraries of cloned *Z. tritici* effectors that were screened to identify effector candidates with putative pathogen-associated molecular pattern (PAMP)-triggered immunity (PTI)-suppressing activity. The effectors from each library were transiently expressed in *Nicotiana benthamiana*, and expressing leaves were treated with bacterial or fungal PAMPs to assess the effectors' ability to suppress reactive oxygen species (ROS) production. From these screens, numerous effectors were identified with PTI-suppressing activity. In addition, some effectors were able to suppress cell death responses induced by other *Z. tritici* secreted proteins. We used structural prediction tools to predict the putative structures of all of the *Z. tritici* effectors and used these predictions to examine whether there was enrichment of specific structural signatures among the PTI-suppressing effectors. From among the libraries, multiple members of the killer protein-like 4 (KP4) and killer protein-like 6 (KP6) effector families were identified as PTI suppressors. This observation is intriguing, as these protein families were previously associated with antimicrobial activity rather than virulence or host manipulation. This data provides mechanistic insight into immune suppression by *Z. tritici* during infection and suggests that, similar to biotrophic pathogens, this fungus relies on a battery of secreted effectors to suppress host immunity during early phases of colonization.

KEYWORDS
fungal pathogens, heterologous expression, protein structural families, PTI, wheat

1 | INTRODUCTION

Zymoseptoria tritici is a major fungal pathogen of wheat, particularly in Europe, and is responsible for Septoria tritici blotch (STB) disease (Fones & Gurr, 2015; Torriani et al., 2015). This fungus is unusual in that it undergoes an extended latent asymptomatic growth phase that can last over 2 weeks under field conditions. During this phase, the fungus grows epiphytically on wheat leaf surfaces before invading leaves through open stomata and growing through the apoplastic space of the mesophyll (Fantozzi et al., 2021; Sánchez-Vallet et al., 2015). Throughout this phase, there is minimal activation of host defences. The fungus then transitions to necrotrophy, which is accompanied by the appearance of macroscopic disease symptoms and death of host cells. While the fungus is infecting the host, the host expresses membrane-associated receptors that monitor the apoplastic space for pathogen-associated molecular patterns (PAMPs), such as bacterial flg22 or fungal chitin, or specific effectors. Upon recognition of these foreign elements, the receptors signal for PAMP-triggered immunity (PTI) or effector-triggered immunity (ETI), respectively (Dodds & Rathjen, 2010; Kanyuka & Rudd, 2019). Accordingly, it is assumed that during the asymptomatic phase, *Z. tritici* secretes effectors into the apoplastic space to suppress PTI and ETI (Stotz et al., 2014; Tian et al., 2021).

Although hundreds of effector proteins have been predicted computationally from genome and transcriptome data (Gohari et al., 2015; Haueisen et al., 2019; Rudd et al., 2015), only a few have been functionally characterized. The effectors *AvrStb6*, *AvrStb9*, and *Avr3D1* have been shown to trigger ETI responses on the wheat with resistance genes *Stb6*, *Stb9*, and *Stb7/Stb12*, respectively (Amezrou et al., 2023; Meile et al., 2018; Zhong et al., 2017). AvrStb9 contains a protease domain, and it is speculated that this domain contributes towards its virulence function. However, the functions of AvrStb6 and Avr3D1 have yet to be demonstrated. Another effector, ZtSSP2, has been demonstrated to interact with a wheat E3-ubiquitin ligase and this interaction is hypothesized to suppress PTI responses (Karki et al., 2018), though this hypothesis remains to be conclusively proven. The most well studied are the LysM domain-containing effectors, which sequester free chitin before it is recognized by the host and offer a protective coat to hyphae from host-secreted chitinases (Marshall et al., 2011; Sánchez-Vallet et al., 2020; Tian et al., 2021). Via this mechanism, the pathogen can mask its own presence and evade host defences. However, *Z. tritici* mutants lacking LysM domain effectors remain partially virulent, suggesting the existence of other immune-suppressing effectors produced by this fungus. No other *Z. tritici* effectors have been observed as active PTI suppressors.

High-throughput screening of fungal effectors in wheat still has technical difficulties, despite improvements in wheat protoplasts (Saur et al., 2019; Wilson et al., 2024) or via viral expression (Chen et al., 2023). For ease of analysis, we chose to screen the effectors in the model organism *Nicotiana benthamiana*. Perception of PAMPs and apoplastic effectors often relies on the activity of cell-surface receptor-like proteins (RLPs) or receptor-like kinases (RLKs). In many cases, receptors must partner with other cell-surface co-receptors such as BRASSINOSTEROID INSENSITIVE 1-associated receptor kinase 1 (BAK1) or Suppressor of BIR1-1/EVERSHED (SOBIR1/EVR) to initiate defence signalling (Liebrand et al., 2013). We hypothesized that *Z. tritici* effectors that suppress conserved immune responses, such as BAK1-dependent responses, could be identified by screening their immune-suppressing activity in *Nicotiana benthamiana* (i.e., suppression of pathways conserved across monocots and dicots), and that these findings could be later translated into a wheat system. Herein, we describe the independent screening of two different *Z. tritici* effector libraries, transiently expressed in *N. benthamiana*, to identify novel *Z. tritici* effectors with putative functions in suppression of PTI and ETI defence responses.

2 | RESULTS

2.1 | Eleven candidate effectors selected as preliminary candidates for PTI suppression

In this study, two libraries of effectors were examined, with different gene name identifiers (Goodwin et al., 2011; Grandaubert et al., 2015). The identifiers for each effector from both naming conventions (https://mycocosm.jgi.doe.gov; Goodwin et al., 2011, 10.1534/g3.115.017731, Grandaubert et al., 2015) are listed in File S1. Both effector libraries were composed of full-length effector sequences, with native promoters to stay comparable with the previous screening study in *N. benthamiana* (Kettles et al., 2017). We first selected candidate effectors to establish our screen according to two main criteria: First, we considered that PTI-suppressing effectors would show conservation among *Zymoseptoria* spp. as they are targeting core immune signalling processes. Second, we hypothesized that PTI-suppressing effectors would be specifically up-regulated during early plant colonization.

We first explored genomic data from five different *Zymoseptoria* species (*Z. tritici*, *Z. ardabiliae*, *Z. brevis*, *Z. passerinii*, and *Z. pseudotritici*) to identify conserved orthologous effector candidates. We included genome data from three *Z. tritici* isolates (Zt05, Zt09 [synonymous with IPO323], and Zt10) (Grandaubert et al., 2015; Haueisen et al., 2019), considering that some effector genes can show presence–absence variation among individuals within the same species. We designed our analyses to identify orthologous genes present in all the analysed genomes. To this end, we performed an orthologue clustering analysis to identify shared effector orthogroups (1e−5 cut-off) resulting in 56 orthogroups among the eight *Zymoseptoria* genomes (File S1).

Based on available RNA-seq data, we next selected *Z. tritici* (Zt09) orthologues from the 56 conserved orthogroups that were expressed during the symptomless growth phase (Haueisen et al., 2019). Twenty-one effector candidates were highly expressed during the symptomless phase of infection (Table 1). Eleven

TABLE 1 Zt09 orthologues of effectors shared among all *Zymoseptoria* spp. that are highly expressed in either the necrotrophic or symptomless life stages (FPKM values).

Effector library 1					
Effector ID	3 DPI	7 DPI	13 DPI	20 DPI	Predicted protein domain
Zt09_chr_5_00190	3.000	964.000	174.000	21.000	No
Zt09_chr_1_01278	2.353	1346.820	388.747	16.238	No
Zt09_chr_1_02089	2784.040	1130.830	351.267	679.491	No
Zt09_chr_1_01276	24.213	800.271	249.882	24.867	No
Zt09_chr_4_00056	107.524	1085.190	1203.230	70.107	No
Zt09_chr_4_00469	25.878	475.242	914.117	361.181	No
Zt09_chr_8_00412	26.453	430.079	232.957	26.103	LysM (Chen et al., 2023; Goodwin et al., 2011)
Zt09_chr_1_00132	0	330.243	115.889	6.076	No
Zt09_chr_7_00276	425.071	695.194	602.686	596.913	Cyclophilin-like
Zt09_chr_2_00242	43.248	219.234	116.208	39.932	Hce2 (Kettles et al., 2017)
Zt09_chr_10_00356	123.602	124.803	86.445	109.563	Duf2012
Zt09_chr_3_00610	254.108	1061.490	677.792	324.428	Ribonuclease (Kettles et al., 2018)
Zt09_chr_6_00044	390.542	215.367	101.428	65.288	PR1-like
Zt09_chr_3_00904	7.177	3079.040	1092.280	77.793	No
Zt09_chr_3_00971	8.880	1138.540	623.621	18.977	Arabfuran-catal
Zt09_chr_1_00805	0	43.218	3.891	0.784	No
Zt09_chr_12_00080	192.981	223.174	193.916	175.779	EMP24
Zt09_chr_3_00667	13.644	96.777	343.599	23.132	No
Zt09_chr_5_00497	192.017	175.528	80.582	120.353	FAS1
Zt09_chr_2_01151	35.845	19.719	984.238	328.263	Cutinase

Note: Dark green = highest expression time-point, light green = second highest expression time-point. Gene models and accessions are from Jumper et al. (2021) and FPKM values are from Couto and Zipfel (2016).

Abbreviation: DPI, days post-infection.

candidates were most highly expressed during the necrotrophic phase, and 34 effectors displayed negligible expression during any phase of infection. We considered the 21 effectors as putative candidates that could suppress the PTI during the asymptomatic infection (File S1).

We used InterProScan (Jones et al., 2014) to add functional annotations to the 21 effector candidates. Ten effectors had predicted protein domains not including HCE2, an effector-associated domain derived from *Cladosporium* Ecp2 effectors (Lauge et al., 1998; pfam: PF14856). Among these, we identified the previously characterized Zt6, a secreted ribonuclease with antimicrobial and cell death-inducing activity (Kettles et al., 2018), and also a LysM-domain-containing effector, underlining the suitability of our approach to identify functionally relevant genes (Table 1). Finally, we identified 11 symptomless phase-expressed effectors without known protein domains (with the exception of the HCE2 domain), and we focused our analyses on these unknown candidates (intraspecific variation among these candidate effectors listed in File S1).

2.2 | Five *Z. tritici* effector candidates suppress the flg22-induced PTI response

We then screened the 11 candidate effectors in *N. benthamiana*, to assess their ability to suppress a PAMP-triggered reactive oxygen species (ROS) burst, using the potent elicitor, flg22.

To establish an appropriate positive control for the assay, we surveyed orthologues of a known PTI-suppressing effector NIS1 identified in *Magnaporthe oryzae* (MoNIS1) (Irieda et al., 2019). Not only *Z. tritici* but also other *Zymoseptoria* sister species encoded orthologues of MoNIS1 (identified via BLASTp searches, File S1). In particular, *Z. tritici* IPO323 had two homologues, with only one expressed during the asymptomatic phase of infection (File S1). We hypothesized that this protein (hereon described as ZtNIS1) would similarly inhibit PTI in *N. benthamiana*, akin to MoNIS1's action.

In our transient gene expression assay, a control was expressed on the left half of the leaves, while the comparison group was expressed on the right half to minimize biological variations that can arise from differences between and within leaves. The relative

luminescence accumulation (RLU) for comparison groups was measured with respect to the control from the same leaf after flg22 treatments. We selected the hell-fire tag (HF tag), with an added fungal signal peptide, as our negative control. When the negative controls were expressed in both halves of the leaves and PTI was induced with flg22, the RLU values were approximately 1 (Figure 1), indicative of no PTI suppression. We then tested ZtNIS1 and MoNIS1 by transiently expressing each of these effectors on the right half of the leaves. The RLU values for MoNIS1 and ZtNIS1 were significantly lower than the control experiment (Figure 1), confirming that ZtNIS1 has a similar PTI-suppressing activity as MoNIS1 and can serve as a positive control.

Validating positive and negative controls in our assays, we assessed the suppressive ability of each of the 11 effectors on flg22-induced ROS burst in *N. benthamiana* (Figure 1). One of the effectors, Zt_3_00667, induced cell death and was therefore excluded. Among the remaining 10 effector candidates screened, five displayed significantly reduced RLU and were identified as putative suppressors

of flg22-induced ROS burst. These effectors were Zt_1_1278, Zt_1_132, Zt_5_190, Zt_3_904, and Zt_2_242. Among the observed immune suppressors, Zt_1_132, displayed the weakest suppressive phenotype, with an average RLU of 0.88. The remaining suppressors have a greater magnitude of suppression, more similar to ZtNIS1.

2.3 | Additional *Z. tritici* candidate effectors suppress flg22-, β-glucan-, or chitin-triggered immunity when transiently expressed in *N. benthamiana*

Our initial screen indicated that five out of 11 tested candidate effectors suppressed the flg22-induced ROS burst. This relatively high incidence prompted us to question whether ROS burst suppression might be a common feature of *Z. tritici* effectors. To assess the prevalence of this phenomenon, we made use of an established library of cloned *Z. tritici* candidate effectors to uncover
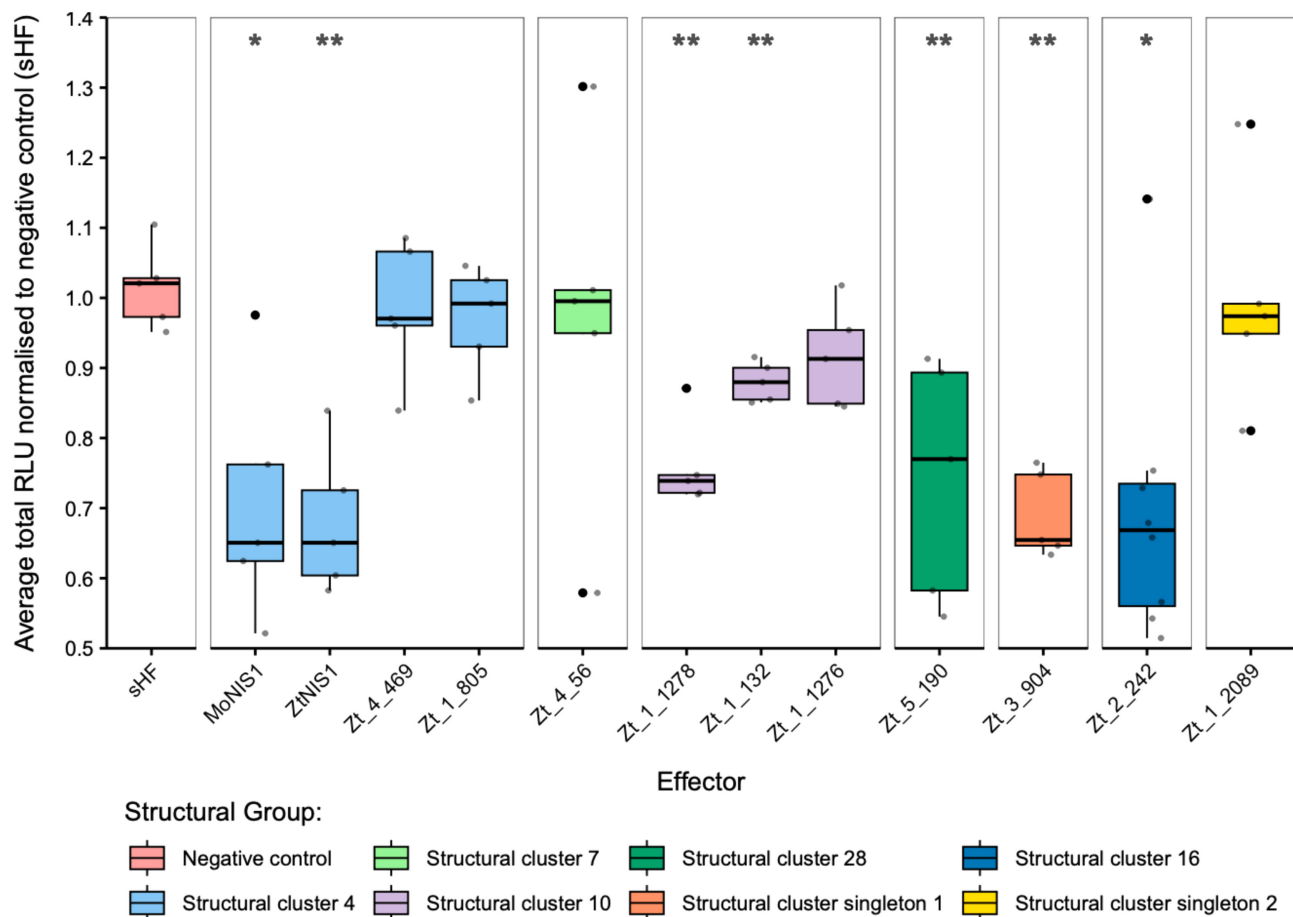

FIGURE 1 Various effectors from *Zymospetoria tritici* consistently suppress flg22-induced reactive oxygen species (ROS) burst. Candidate effectors were transiently expressed in *Nicotiana benthamiana*, with *Agrobacterium*. Each leaf had the negative control (sHF) expressed on one half and an effector on the other half. At 72 h post-infiltration, leaf discs from each side of a leaf were treated with flg22. The average total relative luminescence (RLU) from all of the leaf discs in each ROS burst assay was measured by comparing the total luminescence of effector-expressing leaf discs to the negative control (sHF). Individual experiments were performed five times, represented by the five datapoints in each plot. For Zt_2_242 there was one non-conforming data point. To confirm that this was an outlier, an additional three repeats were performed (i.e., a total of eight data points). Five effectors were identified as significant suppressors of flg22-induced ROS burst in comparison to the sHF controls (Wilcoxon test: *$p < 0.05$, **$p < 0.01$).

additional PTI-suppressing proteins. This second library contains 48 effectors that were identified as exhibiting elevated expression during the symptomless and transition phases of wheat leaf colonization (Table 2) (Kettles et al., 2017, 2018; Rudd et al., 2015; Welch et al., 2022). Each was previously cloned into an *Agrobacterium tumefaciens* expression vector (Kettles et al., 2017). These effectors were not shown to induce cell death in *N. benthamiana* and their virulence functions are currently unknown. These 48 candidate

effectors were transiently expressed in *N. benthamiana* and tested for ability to suppress the ROS burst induced by either flg22 or the fungal PAMPs chitin and β-glucan (laminarin).

In this screen, we used a secreted GFP (sGFP) as a negative control for ROS suppression, and the *Pseudomonas syringae* effector AvrPtoB (expressed intracellularly) was used as a positive control. In experiments with all three PAMPs, RLU values for AvrPtoB were consistently and significantly lower than the sGFP-expressing leaf

TABLE 2 Library of 48 *Zymoseptoria tritici* effectors expressed in *Nicotiana benthamiana* (Lauge et al., 1998) (FPKM values).

Effector library 2

Effector ID	1 DPI	4 DPI	9 DPI	14 DP	21 DPI	Predicted protein domain
103555	71.827	31.907	1471.730	780.445	26.631	No
106127	34.303	38.546	109.881	33.776	21.095	No
88698	252.613	270.297	741.601	84.582	0.684	No
67799	436.424	516.756	2230.690	281.550	4.512	No
90776	44.436	68.721	1218.650	884.560	77.272	No
103650	21.289	38.481	159.504	40.033	12.543	FAS1
91702	4.106	0	6.667	91.141	2.516	NTF2-like
91885	6.557	2.119	31.174	17.754	3.209	No
103900	133.184	394.016	4052.550	595.846	8.835	No
92097	651.416	16.966	190.100	32.776	160.149	Cellulase
104000	439.149	534.497	871.931	493.021	24.822	No
92792	527.669	8.461	13.295	5.094	1.905	No
104404	498.735	496.239	3676.130	918.011	4.634	No
93075	368.975	628.317	2148.160	116.477	4.206	No
104794	1371.450	548.493	1995.370	2316.030	185.178	No
94107	36.729	8.798	75.338	29.269	3.531	No
110052	10.238	14.733	75.898	10.648	1.149	No
94290	0	18.650	85.282	700.585	0.033	No
94526	110.308	218.860	1327.450	513.034	200.947	No
95478	11.674	11.121	231.658	102.245	7.549	No
105826	200.536	80.384	178.797	66.016	5.860	No
96868	37.439	31.517	189.966	197.665	60.399	AltA1 (Lu & Faris, 2019)
106436	7.559	238.087	478.146	17.871	0.663	No
30802	68.628	120.417	188.117	136.372	4.498	Metalloprotease
34332	33.064	43.739	42.518	40.095	49.460	Virginiamycin B lyase
70022	8.065	5.704	5.817	3.848	2.472	No
71681	36.652	32.122	93.288	50.386	10.761	Cellulase
79286	24.363	15.857	33.593	13.595	13.910	No
82936	3.894	4.667	3.363	5.413	6.675	Cupredoxin
89734	25.457	46.662	9.693	7.203	5.944	No
91285	2.197	0	0	3.992	1.174	No
91662	4.706	315.802	1610.740	21.874	0	No
94383	11.825	52.356	268.536	41.362	15.931	No
95416	282.183	135.761	513.047	98.152	8.267	No
95491	0	29.006	7.675	14.475	197.868	Hydrophobin

(Continues)

TABLE 2 (Continued)

Effector library 2					
Effector ID	1 DPI	4 DPI	9 DPI	14 DP	21 DPI	Predicted protein domain
95831	83.715	22.991	223.016	52.464	9.662	No
96389	57.431	0	121.407	96.156	8.396	No
96543	147.111	722.166	79.007	12.489	6.654	Hydrophobin
96865	2.161	0	98.196	42.474	2.096	No
97449	566.005	493.830	2595.600	300.374	1.074	No
97526	0	60.286	316.687	14.418	1.215	No
102996	75.306	97.742	16.206	19.136	104.235	No
104383	674.260	470.608	2172.050	287.264	28.716	No
104444	146.918	1677.160	10,414.200	1003.580	21.661	No
105867	206.743	175.102	1068.210	244.413	28.646	No
105896	37.615	25.079	265.302	120.271	78.709	No
107904	33.792	114.655	176.197	148.486	12.684	Hce2 (Kettles et al., 2017)
111760	13.623	35.890	189.232	29.099	10.122	No

Note: Dark green = highest expression time-point, light green = second highest expression time-point. Gene models and accessions are from Jones et al. (2014) and FPKM values are from Derbyshire and Raffaele (2023).
Abbreviation: DPI, days post-1infection.

discs, indicating their suitability as controls. Suppression of the flg22-, laminarin-, and chitin-induced ROS bursts were observed for 9, 5, and 13 effectors, respectively (Figure 2). In assays with flg22, the magnitude of ROS suppression by some *Z. tritici* effectors, whilst statistically significant, was weaker than that observed for AvrPtoB (Figure 2a). However, effectors 104404 and 104000 were notable as they suppressed ROS to a level similar to the AvrPtoB positive control. For laminarin-triggered ROS, we observed a suppressive phenotype for five effectors (Figure 2b). Similar to the flg22 assays, the suppressive effect caused by many effectors was less pronounced than by the AvrPtoB positive control, although still statistically significant. Only effector 104404 suppressed laminarin-induced ROS to a similar degree as AvrPtoB. For chitin-triggered ROS, we found a suppressive phenotype for 13 effectors (Figure 2c). In contrast to the other PAMPs, the magnitude of ROS suppression following chitin treatment was often stronger, with several effectors exhibiting a potency similar to that of AvrPtoB. Across experiments, we found that 12 effectors suppressed the ROS burst for a single PAMP, three effectors suppressed ROS induced by two PAMPs, and three effectors suppressed the ROS induced by all three PAMPs tested. This data indicates that ROS suppression is a common feature shared by numerous *Z. tritici* candidate effector proteins.

Given our observations of ROS burst suppression by a different subset of candidate effectors in the present study (Figure 2), we speculated that some of these proteins may have other immunosuppressive functions, including the ability to suppress ETI. We previously reported that several *Z. tritici* candidate effectors induce BAK1/SOBIR1-dependent cell death in *N. benthamiana* (Kettles et al., 2017; Welch et al., 2022). To test this possibility, we co-expressed the cell death-inducing effectors Zt6, Zt9, Zt11, and Zt12 (Kettles et al., 2017, 2018) with the 48 candidate effectors described

above (Figure 3). Co-infiltrations of cell death-inducing proteins with sGFP were performed on the same leaves as controls. In these preliminary experiments, we observed repeated suppression of cell death by six candidate effectors (103900, 30802, 88698, 91885, 92097, and 95478) (Figure 3). All six effectors were able to suppress Zt12-induced cell death, whilst three were also able to suppress Zt9-induced cell death. One effector, 92097, was able to suppress cell death induced by Zt9, Zt11, and Zt12. However, none of the effectors tested were able to suppress Zt6-induced cell death. This is consistent with Zt6 functioning as a ribonuclease toxin that initiates cell death independently of BAK1/SOBIR1 (Kettles et al., 2017). Four of the six cell death-suppressing effectors were previously found to suppress ROS production induced by one or more PAMPs (Figure 3). These initial ROS burst- and cell death-suppression results indicate that *Z. tritici* candidate effectors are able to suppress multiple defence pathways, thus contributing to evasion of immune surveillance.

2.4 | Structural predictions identified conserved folds among PTI-suppressing effectors

Structure prediction algorithms such as AlphaFold (Jumper et al., 2021) can offer novel insights into effectors that lack functional domains and sequence-related homologues. To identify possible commonalities among the PTI suppressors, we clustered the whole proteome of *Z. tritici* IPO323 using structures predicted by AlphaFold (Jumper et al., 2021) (File S1). Where possible, we assigned the effectors of interest to specific structural families (Figure 4; File S1). Among the three effectors (104404, 91885, and 111760) that suppressed the flg22-, laminarin-, and chitin-induced ROS bursts, 104404 was predicted to belong to a killer protein-like
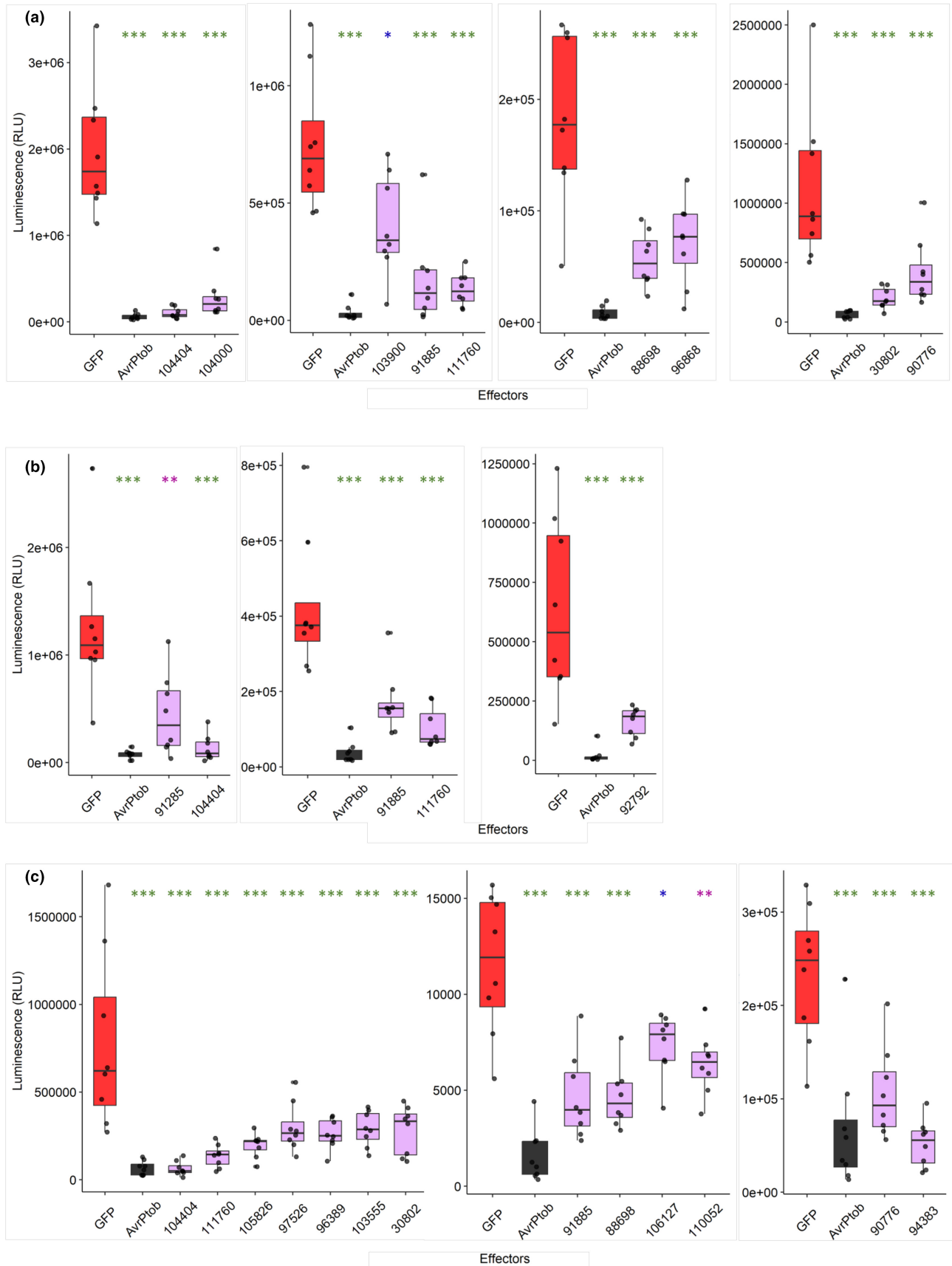
FIGURE 2 Suppression of the flg22-, laminarin-, and chitin-induced reactive oxygen species (ROS) bursts. Candidate *Zymoseptoria tritici* effectors were expressed in *Nicotiana benthamiana* and leaf squares used for ROS assay at 48 hours post-infiltration. sGFP (shown in red) and AvrPtoB (shown in grey) were used as negative and positive controls for ROS burst suppression, respectively. (a) flg22 treatment; (b) laminarin treatment; (c) chitin treatment. Asterisks indicate statistical significance at *$p < 0.05$, **$p < 0.01$, ***$p < 0.001$ as performed by Tukey's HSD test.
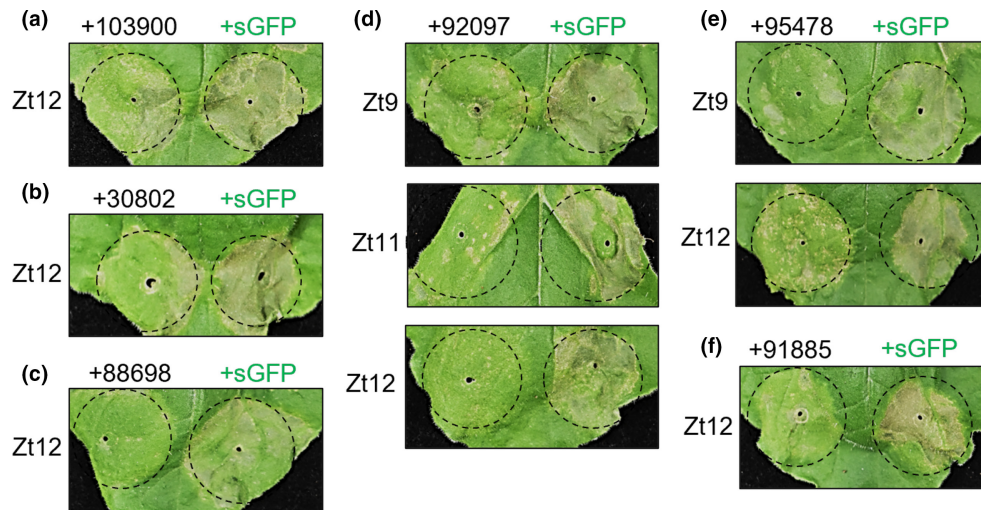
FIGURE 3 Suppression of effector-induced cell death in *Nicotiana benthamiana*. Leaves were co-infiltrated with *Agrobacterium tumefaciens* strains delivering a cell death inducer (Zt6, Zt9, Zt11, Zt12) and either a negative control strain (+sGFP) or a candidate secreted effector (+effector). Effectors shown are (a) 103900, (b) 30802, (c) 88698, (d) 92097, (e) 95478, (f) 91885. Dashed circles indicate co-infiltration pairs where cell death suppression was observed in the effector treatment compared to the sGFP control. Leaves were photographed at 5 days post-infiltration.

4 (KP4-like fold) structural family. A reliable structure was predicted for 91885 with pTM score of 0.723, and it was clustered with two other effectors, 88619 and 106743, not tested in this study; however, no specific family was assigned to this cluster. In contrast, 111760 could not be accurately modelled. Three effectors (88698, 30802, and 90776) suppressed both flg22- and chitin-induced ROS bursts. The effector candidate 88698 belonged to the killer protein-like 6 (KP6-like fold) family, 30802 was predicted to be a metalloprotease based on structural similarity, and 90776 partially matched a pectate-lyase fold.

In addition to 104404, another PTI-suppressing effector, Zt_2_242, was predicted to belong to the KP4 family. Despite sharing similar structures (Figure 4b), these proteins do not share similarity at the sequence level. In total, seven effectors within the *Z. tritici* genome are predicted to belong to the KP4 family of effectors (File S1). Another structural family was identified with multiple PTI-suppressing members. The first of these are the KP6-fold effectors, for which four were identified with varying PTI-suppressing activity. Zt_1_1278 and 88698 are paralogues, and both suppressed the flg22-induced ROS burst. The other two KP6-fold effectors, 105826 and 96389, were not observed to suppress the flg22-induced ROS burst. However, like 88698, they each suppressed the chitin-induced ROS burst. Effectors 105826 and 96389 share no discernible sequence similarity with each other, or with either of 88698 or Zt_1_1278, but are similar in structure (Figure 4c). In total, *Z. tritici* is predicted to have nine KP6-fold effectors (File S1), which includes Zt9, previously found to trigger cell death in *N. benthamiana* and used as a treatment in the cell death-suppression assay (Figure 3).

In addition to 111760, one other effector investigated here for which no specific 3D structure could be predicted, 103900, was identified as a PTI suppressor. This effector is of interest as it was present in both libraries and identified as a suppressor of the

flg22-induced ROS burst in both screens. The amino acid sequences of 111760 and 103900 were independently queried against the NCBI-NR database using BLASTp in order to identify sequence-similar homologues. Homologues of 111760 were found among *Mycosphaerellaceae* species (Figure 4d), whereas 103900 was limited to *Z. tritici* and some *Cercospora* species (File S1).

3 | DISCUSSION

Despite the importance of *Z. tritici* as a major wheat pathogen, relatively little is known about the wheat–*Z. tritici* molecular interactions during the extended symptomless growth phase of infection. Our long-term goal is to identify and characterize effector proteins secreted during *Z. tritici* infection that target and suppress components of the wheat immune system, and in doing so, potentially identify host resistance or susceptibility factors. To support this goal, we established a high-throughput assay allowing us to screen multiple *Z. tritici* effector candidates with the overarching objective to identify immune-suppressing effectors. With our method based on heterologous expression, we were able to identify multiple *Z. tritici* effectors with PTI-suppressing activity. Our findings offer support that *Z. tritici* uses multiple effectors that might enable immune surveillance evasion, beyond the previously described LysM-domain effector family (Sánchez-Vallet et al., 2020; Tian et al., 2021).

It is known that *Z. tritici* suppresses the wheat immune response during infection, and, furthermore, *Z. tritici* infection can lead to systemic induced susceptibility (SIS), enabling non-adapted pathogens or avirulent isolates of *Z. tritici* to co-infect (Bernasconi et al., 2023; Seybold et al., 2020). It is likely that SIS is induced as a result of effector manipulation of the host, for example, by altering long-range hormonal signalling. The receptors that monitor the apoplastic space,
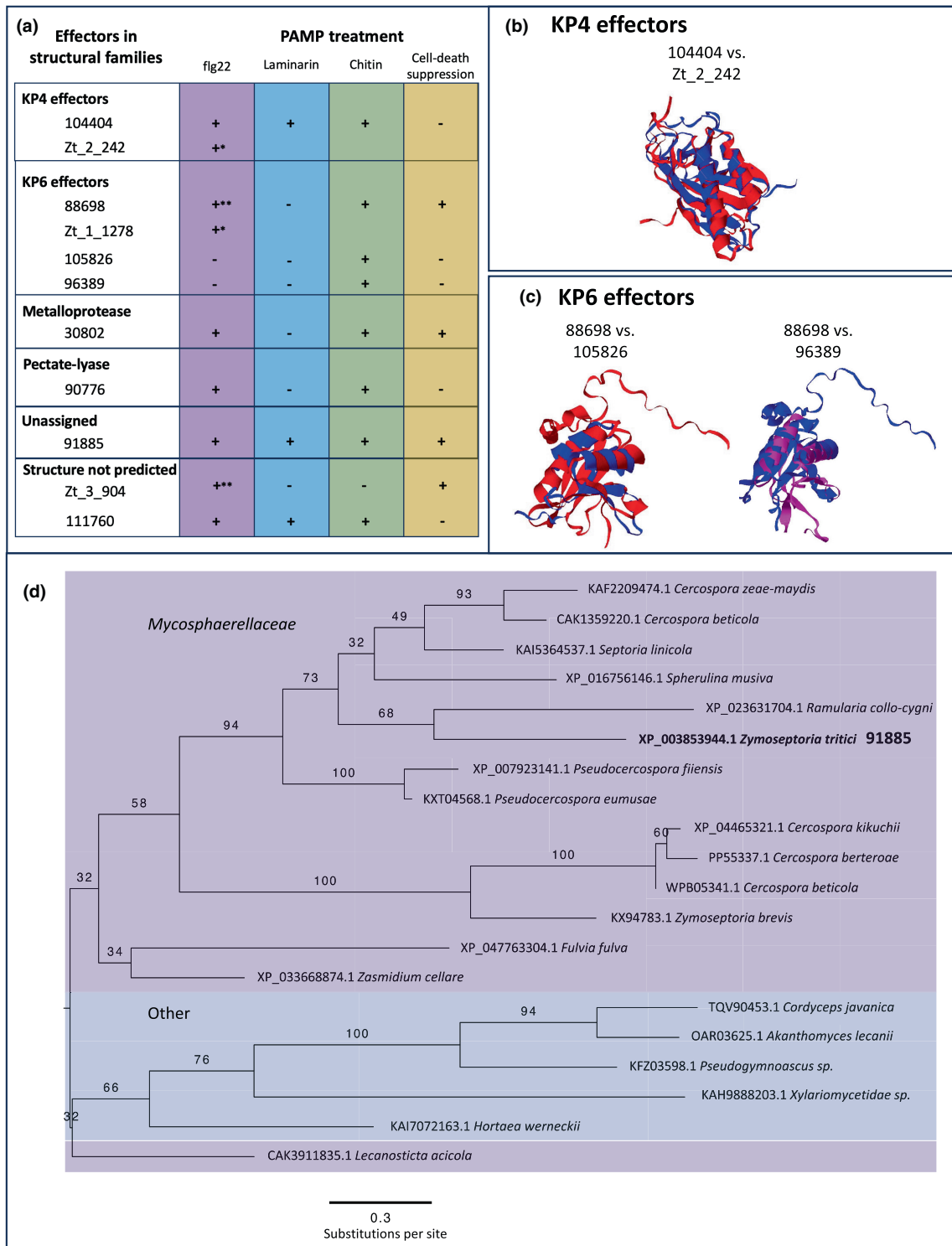
FIGURE 4 Multiple KP4-like fold and KP6-like fold effectors suppress pathogen-associated molecular pattern (PAMP)-triggered immunity responses. (a) Summary of selected effectors, their observed immune-suppressing activity, and predicted structural folds based on AlphaFold. *Only flg22 tested. **Identified in both screens. (b) Structure alignment of the two immune-suppressing KP4-fold effectors (red = 104404; blue = Zt_2_242). (c) Structural alignments of non-paralogous KP6-fold effectors. (d) The structure of 88698 was used as the reference in both alignments (red = 88698; blue = 105826; magenta = 96389. (e) Phylogenetic tree of sequence homologues of 91885 showing the occurrence of homologues across other fungal species.

in which *Z. tritici* resides, can signal for changes in plant hormone and peptide signalling, altering the status of pathogen susceptibility (Couto & Zipfel, 2016; Guo et al., 2018; Zhang et al., 2018; Ziemann et al., 2018). Broadly, therefore, it is important that we study how pathogen effectors can be used to suppress or subvert receptor signalling. To this end, we first examined the function of ZtNIS1 to see

if this *Z. tritici* effector displays similar BAK1-dependent immune-suppressing activity as described from orthologues in *Colletotrichum* and *Magnaporthe* spp. (Irieda et al., 2019). Similar to the orthologues from these two species, the expressed *Z. tritici* homologue of NIS1 can suppress PTI responses. Our subsequent findings demonstrate that ZtNIS1 is not alone, and an array of *Z. tritici* effectors suppress plant immune responses.

Interestingly, we observed that some PTI-suppressing effector candidates share structural folds. The most represented was the KP6 fold, with four PTI-suppressing effectors. KP6-like effectors were first described from yeast as virally encoded proteins with antimicrobial activity. They have subsequently been described from virus-associated maize fungal pathogen, *Ustilago maydis*, with antifungal activity (Allen et al., 2013). A variety of structural prediction screens of plant pathogens found this fold to be well-represented (Derbyshire & Raffaele, 2023; Irieda et al., 2019; Rocafort et al., 2022; Yu et al., 2023), and so, combined with our new data, there is evidence of this fold playing a role in plant–pathogen interactions. Despite our observations of these four *Z. tritici* KP6-fold effectors suppressing PTI, not all members in this structural family do. For example, one of the KP6-fold effectors, Zt9, is known to induce cell death in *N. benthamiana* rather than to suppress immunity; however, this phenotype in *N. benthamiana* does not mean it is not a suppressor in wheat. This effector is one of the nine *Z. tritici* KP6-fold effectors, demonstrating potential variation in activity. KP6-fold effectors from *Cladosporium fulvum* have been screened in wild tomatoes and cell death was observed. It is, therefore, possible that there are solanaceous receptors that recognize members of this structural family (Mesarich et al., 2018). Follow-up analyses should investigate each of these nine *Z. tritici* homologues and determine which are PTI suppressors, which induce cell death, and what is the difference between each that results in these polarized phenotypes.

Surprisingly, two effectors from killer protein-like 4 (KP4) family were also identified with PTI-suppressing activity. KP4-fold effectors have also been described as antimicrobial having a calcium channel-inhibiting activity, when screened against mammalian, fungal, and plant cells (Allen et al., 2013). During PTI, apoplastic calcium is an important signalling molecule and transported into the cell (Wang & Luan, 2024). There is a close association between this PTI calcium signalling and other signalling responses, such as ROS burst (Köster et al., 2022). Therefore, in the cases of the *Z. tritici* KP4-fold effectors, it is quite possible they are attenuating calcium signalling, which in turn results in the observed ROS burst-suppression activity. Previously, a *Z. tritici* KP4-fold effector was identified as a candidate necrosis-inducing effector necrosis-inducing protein 2 (ZtNIP2; not screened in this study) from culture filtrate of the fungus (M'Barek et al., 2015). Four *Fusarium graminearum* KP4-fold effectors have been described with putative roles in virulence in wheat (Lu & Faris, 2019). Three of these *F. graminearum* effectors were identified in a cluster, and when the entire cluster was knocked-out, virulence in wheat seedlings was reduced and root development inhibited (Lu & Faris, 2019). These previous findings, combined with our own, indicate a potentially important role for KP4-fold effectors in plant

infection (aside from niche competition between fungi and other microbes).

Although we have chosen to highlight effectors belonging to specific and enriched effector fold families, multiple effectors were identified with putative immune-suppressing activity from among our two libraries. For example, 91885, displayed PTI-suppressing activity for all treated PAMPs in our assays and appears to be a conserved effector among the *Mycosphaerellaceae* (and clustered with two other *Z. tritici* effectors, 88619 and 106743). These effectors identified are all interesting candidates for downstream functional analyses, and their unscreened structural homologues should be examined for whether they possess similar immune-suppressing activity. However, we should emphasize that effector structural predictions are very useful for hypothesis generation but should not be used to conclude specific function without validation.

It should also be noted that our findings were obtained via screening in *N. benthamiana*. *N. benthamiana* is a useful model for studying effector function due to ease of use for both *Agrobacterium* infiltration and testing immune responses. Hereby, several new studies have demonstrated the use of heterologous expression to characterize the role of plant pathogen effectors from *Z. tritici* and related species (Gomez-Gutierrez et al., 2023; Zhao et al., 2023). However, this is still a non-host system in which the effectors were expressed with their native signal peptides, which may have hindered processing to the apoplast. As such, the activity of the *Z. tritici* effectors identified here should ideally be corroborated in wheat protoplasts or with viral expression in whole wheat plants, with wheat signal peptides. Similarly, our presented cell death results are qualitative observations performed to support our quantitative ROS burst assays. Although reproducible, we cannot conclusively exclude variation among infiltrations. We aim to expand upon these initial observations in future studies, and also to ascertain why certain effectors suppress specific immune response phenotypes.

Our findings suggest that immune suppression during the symptomless infection stage is an important part of colonization. This is a relatively cryptic stage of growth, and there is no evidence of *Z. tritici* feeding (Chen et al., 2023; Sánchez-Vallet et al., 2015). This emphasizes the importance of the symptomless phase, developmentally, for the fungus and, accordingly, the importance of evading the host immune system. Most of the effectors examined in this study are primarily expressed during the symptomless phase; however, host recognition can occur earlier, during initial stomatal penetration. The avirulence effector *AvrStb6* is expressed during stomatal penetration. In wheat cultivars with AvrStb6's corresponding resistance receptor, Stb6, infection is hindered at this early stage when the fungus grows through the stomatal opening (Alassimone et al., 2024; Noei et al., 2022). A similarly timed phenotype is observed for another resistance to *Z. tritici* receptor Stb16q (Battache et al., 2022). These avirulence interactions all occur before the immune-suppressing effectors identified in this study are highly expressed. It is relevant to note that infection of a virulent strain of *Z. tritici* can enable subsequent infection

of an independently avirulent strain, by inducing SIS (Bernasconi et al., 2023; Seybold et al., 2020). Therefore, it is quite possible that the timing of immune-suppressing effectors plays an important role in SIS development and inhibition of resistance gene function.

4 | EXPERIMENTAL PROCEDURES

4.1 | Selection of candidate effectors

Candidate gene sets were selected and defined in two independent ways. Firstly, to conduct an initial screen, we selected candidate genes according to expression pattern and sequence conservation across different *Zymoseptoria* species. Total protein sets were obtained for the three *Z. tritici* isolates (Zt05, Zt09, Zt10) (Haueisen et al., 2019). Predicted proteins of *Z. ardabiliae* (Za17) (Stukenbrock et al., 2012), *Z. pseudotritici* (Zp13) (Stukenbrock et al., 2012), and *Z. brevis* (Zb18110) (Grandaubert et al., 2015) were obtained from the JGI Mycosm portal (Za17: https://mycocosm.jgi.doe.gov/Zymar1/Zymar1.home.html; Zp13: https://mycocosm.jgi.doe.gov/Zymps1/Zymps1.home.html; Zb18110: https://mycocosm.jgi.doe.gov/Zymbr1/Zymbr1.home.html). The protein set for *Z. passerini* was derived from the annotation presented in Fuertey et al. (2020).

Effectors from each protein set were predicted with the use of SignalP (v. 5.0b) (Armenteros et al., 2019) and EffectorP (v. 2.0) (Sperschneider et al., 2018). Fasta files for predicted effectors are stored in the Zenodo page associated with this project (10.5281/zenodo.10037259). OrthoMCL predictions were performed with default settings (e−0.5). Input effector fasta files with edited names compatible with OrthoMCL and the OrthoMCL output files are deposited in the same Zenodo page (10.5281/zenodo.10037259). Effector gene expression for early colonization (3 days post-infection [DPI]), asymptomatic growth (7 and 13 DPI), and necrotrophic phase (20 DPI) was obtained from the dataset generated in Haueisen et al. (2019). Candidate effector expression levels were examined for the reference strain Zt09 (synonymous with IPO323). All of the effector candidates and corresponding annotations are listed in File S1 (including amino acid sequences).

Effector protein sequences were analysed with the InterProScan Geneious plug-in (v. 2) (Jones et al., 2014) to predict protein domains. Similarly, phylogenetic analyses were performed using the RAxML Geneious plug-in (v. 4) (Stamatakis, 2006), with a parsimony random seed value of 1234 and 100 bootstrap replicates.

4.2 | Clustering predicted structures

We aimed to cluster the predicted structures of the whole proteome of *Z. tritici* IPO323. A total of 10,689 predicted structures of *Z. tritici* IPO323 (taxonomy ID: 336722) were downloaded from the AlphaFold Database (Varadi et al., 2022). The structures of 992 secreted proteins were obtained from the previous study and

replaced the models from the AlphaFold database if their averaged pLDDT scores were higher than the database structures (Seong & Krasileva, 2023). This corresponded to 849 structures. The structures of three proteins (Zt_1_805, Zt_1_1278, and Zt_9_367), missing in *Z. tritici* IPO323, were predicted with AlphaFold v. 2.3.2 and included (Jumper et al., 2021).

Signal peptides predicted from SignalP v. 5.0 were removed from the database structures. Low-confidence N- and C-terminal flexible stretches were trimmed off by examining the average pLDDT with a sliding window of 4 and a cut-off of 40. If the length and the average pLDDT scores of the remaining protein sequences were smaller than 50 amino acids or less than 60, respectively, the structures were discarded. The remaining 8335 structures were clustered with FoldSeek (easy-cluster -s 7.5 -c 0.4 –alignment-type 1 –tmscore-threshold 0.5) (van Kempen et al., 2024). This clustering output was compared to the one from the previous study (Seong & Krasileva, 2023).

4.3 | Candidate effector synthesis and cloning

Full-length effector DNA sequences (intronless) (from isolate Zt09) and Zt_13_171 signal peptide (for entry into destination vector to create the secreted tag) were synthesized as gene fragments by TWIST Biosciences. Sequences were codon optimized for *N. benthamiana* expression and synthesized with sequence overhangs compatible with BsaI cloning into the final vector plasmids (Effector sequences, with BsaI compatible overhangs for entry into the vector plasmid via GoldenGate cloning listed in File S1). The vector plasmid pICSL22011 (with his/FLAG 'hell-fire' tag [HF tag]) was kindly provided by Mark Youles (Synbio). Sequences were cloned into the vectors using the one-pot GoldenGate cloning method, using BsaI. Cloning product was transformed via heat shock into chemically competent *Escherichia coli* Top10 cells for plasmid propagation. Plasmid inserts were Sanger sequenced by Eurofins Genomics (Ebersberg, Germany), using primers from outside the insert site (File S1).

4.4 | Transient expression assays in *N. benthamiana*

Plasmids generated for the construction of either effectors or control sequence (secreted hell-fire tag [sHF]) were transformed into *A. tumefaciens* GV3101 and grown on solid DYT medium (kanamycin [Km], gentamicin [Gm], and rifampicin [Rf] selection) at 28°C for 2 days. Single colonies were selected and grown in liquid DYT (Km+Gm+Rf selection) overnight, at 200 rpm, at 28°C. Glycerol stocks were made from these cultures and stored at −80°C. Before *N. benthamiana* transformation, bacterial glycerol stocks were plated onto DYT (Km+Gm+Rf selection) overnight at 28°C. *Agrobacterium* was scraped from plate into infiltration buffer (IB: 10 mM MgCl₂-MES, acetosyringone), and incubated at room temperature for 1 h. The OD_{600} was measured after 1 h, and diluted in IB to a final OD_{600} of 0.5 (except for p19 silencing

suppressor [kindly provided by M. Sauter, CAU, Kiel], which was included in every assay sample, at an OD_{600} of 0.1). *Agrobacterium* was infiltrated into 4- to 5-week-old *N. benthamiana* leaves using a needleless 1 mL syringe. For experiments performed at the University of Birmingham (Figures 2 and 3), *A. tumefaciens* GV3101 strains harbouring pEAQ-HT-DEST3 (effector) have been described previously. The pEAQ-HT-DEST3 (sGFP) strain was generated in this study by generating a pEAQ-HT-DEST3 construct harbouring the *Nicotiana tabacum* PR1a signal peptide (SP) fused to green fluorescent protein (GFP). For ROS burst assays, all *Agrobacterium* strains were syringe infiltrated into leaves of 4- to 5-week-old plants at an $OD_{600} = 1.2$. For cell death suppression assays, all strains were prepared to an $OD_{600} = 1.8$ and mixed in a 1:1 ratio such that the final concentration of elicitor and sGFP/effector was $OD_{600} = 0.9$. Each experiment was performed three times (sGFP) or pEAQ-HT-DEST3 (AvrPtoB) were infiltrated into leaves at a final $OD_{600} = 1.2$.

4.5 | Elicitor-induced ROS burst suppression assays

For the initial method development, we used 4- to 5-week-old *N. benthamiana* leaves. These were infiltrated with *A. tumefaciens* (one half of a leaf expressing sHF and the other half an effector candidate). Three days post-infiltration, 36 leaf discs were harvested from each side of the leaf and placed in a white-bottomed 96-well plate (sHF leaf discs were placed in wells in rows A, C, and E, and effector leaf discs were placed in rows B, D, and F), in 200 μL of Milli-Q water. The plates were placed in the dark until use (6–9 h). At 20–40 min before measurements, the 200 μL of water was replaced with 100 μL of Milli-Q water. Just prior to reading, leaf discs in rows 11 and 12 were treated with mock (20 μM luminol and 1 μg horseradish peroxidase [HRP]) and leaf discs in rows 1 to 10 were treated with flg22 (12.5 nM flg22, 20 μM luminol and 1 μg HRP, final concentration). Resulting RLU was measured over 30 min in a 200 Pro plate reader (Tecan). Total RLU of the effector-expressing leaf discs was measured as a ratio of the negative control leaf discs' total RLU. Five biological repeats were performed for each effector (eight biological repeats were performed for Zt_2_242). Temperature ranges of the plate reader used in these assays were from 20 to 26°C (below 20°C the ROS burst was reduced and above 26°C the ROS burst values were inconsistent, with leaf discs ranging from highly active to nonresponsive).

For the screening of 48 additional effector candidates at the University of Birmingham, the following methods were used for elicitor treatments. Leaf squares approximately 3 × 3 mm were harvested from 5-week-old *N. benthamiana* plants with a scalpel and added to wells of 96-well plates containing 200 μL deionized water. Plates were incubated in the dark overnight prior to performing the ROS burst assay. The following day, the deionized water in each well was removed immediately prior to the assay, and replaced with 150 μL of assay solution containing HRP (20 ng/mL), luminol L-012 (20 μM), and either flg22 (100 nM), chitin (100 μg/mL), or laminarin (100 μg/mL). Luminescence was captured over 2 h (90 cycles) using a PHERAstar FS plate reader (BMG Labtech) controlled through the PHERAstar control software. Each plate contained eight replicates of each effector or control treatment. These experiments were repeated three times.

CONFLICT OF INTEREST STATEMENT

The authors do not have any conflicts of interest related to this manuscript.

DATA AVAILABILITY STATEMENT

Datasets (predicted effector sets, OrthoMCL output data, and raw and curated ROS burst data sets, structural prediction data) have been uploaded to the project's Zenodo page (DOI: 10.5281/zenodo.10037259) and/or in File S1. Within this Zenodo page, we have also included IP/MS data for ZtNIS1, performed in *N. benthamiana*, identifying putative interaction partners. All plasmids (effector *N. benthamiana* expression plasmids and Y2H plasmids) are available upon request (for material transfer agreements relating to use of pICSL22011 plasmids, please contact Mark Youles, SynBio, The Sainsbury Laboratory, Norwich, UK). Use of the pEAQ-HT-DEST vector system is done so under licence from Plant Bioscience Ltd/Leaf Systems International Ltd (Norwich, UK) to G.K. (University of Birmingham).

ORCID

Elisha Thynne https://orcid.org/0000-0002-6267-9114
Kostya Kanyuka https://orcid.org/0000-0001-6324-4123
Graeme J. Kettles https://orcid.org/0000-0003-1230-9024

REFERENCES

Alassimone, J., Praz, C. Lorrain, C., De Francesco, A., Carrasco-Lopez, C., Faino, L., et al. (2024), The *Zymoseptoria tritici* avirulence factor AvrStb6 accumulates in hyphae close to stomata and triggers a wheat defense response hindering fungal penetration. *bioRxiv*. https://doi.org/10.1101/2024.01.11.575168. [Preprint].

Allen, A., Islamovic, E., Kaur, J., Gold, S., Shah, D. & Smith, T.J. (2013) The virally encoded killer proteins from *Ustilago maydis*. *Fungal Biology Reviews*, 26, 166–173.

Amezrou, R., Audeon, C., Compain, J., Gelisse, S., Ducasse, A., Saitenac, C. et al. (2023) A secreted protease-like protein in *Zymoseptoria tritici* is responsible for avirulence on *Stb9* resistance gene in wheat. *PLoS Pathogens*, 19, e1011376.

Armenteros, J.J.A., Tsirigos, K.D., Sonderby, C.K., Peterson, T.N., Winther, O., Brunak, S. et al. (2019) SignalP 5.0 improves signal peptide predictions using deep neural networks. *Nature Biotechnology*, 37, 420–423.

Battache, M., Lebrun, Marc-Henri, L., Sakai, K., Soudiere, O., Cambon, F., Langin, T. et al. (2022) Blocked at the stomatal gate, a key step of wheat *Stb16q*-mediated resistance to *Zymoseptoria tritici*. *Frontiers in Plant Science*, 13, 921074.

Bernasconi, A., Lorrain, C., Flury, P., Alassimone, J., McDonald, B.A., Sánchez-Vallet, A. et al. (2023) Virulent strains of *Zymoseptoria tritici* suppress the host immune response and facilitate the success of avirulent strains in mixed infections. *PLoS Pathogens*, 19, e1011767.

Chen, H., King, R., Smith, D., Bayon, C., Ashfield, T., Torriani, S. et al. (2023) Combined pangenomics and transcriptomics reveals core and redundant virulence processes in a rapidly evolving fungal plant pathogen. *BMC Biology*, 21, 24.

Couto, D. & Zipfel, C. (2016) Regulation of pattern recognition receptor signalling in plants. *Nature Reviews Immunology*, 16, 537–552.

Derbyshire, M.C. & Raffaele, S. (2023) Surface frustration re-patterning underlies the structural landscape and evolvability of fungal orphan candidate effectors. *Nature Communications*, 14, 5244.

Dodds, P.N. & Rathjen, J.P. (2010) Plant immunity: towards an integrated view of plant–pathogen interactions. *Nature Reviews Genetics*, 11, 539–548.

Fantozzi, E., Kilaru, S., Gurr, S.J. & Steinberg, G. (2021) Asynchronous development of *Zymoseptoria tritici* infection in wheat. *Fungal Genetics and Biology*, 146, 103504.

Fones, H. & Gurr, S. (2015) The impact of *Septoria tritici* blotch disease on wheat: an EU perspective. *Fungal Genetics and Biology*, 79, 3–7.

Fuertey, A., Lorrain, C., Croll, D., Eschenbrenner, C., Freitag, M., Habig, M. et al. (2020) Genome compartmentalization predates species divergence in the plant pathogen genus *Zymoseptoria*. *BMC Genomics*, 21, 588.

Gohari, A.M., Ware, S.B., Wittenberg, A.H.J., Mehrabi, R., M'barek, S.B., Verstappen, E.C.P. et al. (2015) Effector discovery in the fungal wheat pathogen *Zymoseptoria tritici*. *Molecular Plant Pathology*, 16, 931–945.

Gomez-Gutierrez, S. V., Million, C. R., Jaiswal, N., Gribskov, M., Helm, M., Goodwin, S. B., et al, (2023). Mechanisms of infection and response of the fungal wheat pathogen *Zymoseptoria tritici* during compatible, incompatible and non-host interactions. *bioRxiv*. https://doi.org/10.1101/2023.11.20.567875. [Preprint].

Goodwin, S.B., M'barek, S.B., Dhillon, B., Wittenberg, A.H.J., Crane, C.F., Hane, J.K. et al. (2011) Finished genome of the fungal wheat pathogen *Mycosphaerella graminicola* reveals dispensome structure, chromosome plasticity, and stealth pathogenesis. *PLoS Genetics*, 7, e1002070.

Grandaubert, J., Bhattacharyya, A. & Stukenbrock, E.H. (2015) RNA-seq-based gene annotation and comparative genomics of four fungal grass pathogens in the genus *Zymoseptoria* identify novel orphan genes and species-specific invasions of transposable elements. *G3: Genes, Genomes, Genetics*, 5, 1323–1333.

Guo, H., Nolan, T.M., Song, G., Liu, S., Xie, Z., Chen, J. et al. (2018) FERONIA receptor kinase contributes to plant immunity by suppressing jasmonic acid signaling in *Arabidopsis thaliana*. *Current Biology*, 28, 3316–3324.e6.

Haueisen, J., Möller, M., Eschenbrenner, C.J., Grandaubert, J., Seybold, H., Adamiak, H. et al. (2019) Highly flexible infection programs in a specialized wheat pathogen. *Ecology and Evolution*, 9, 275–294.

Irieda, H., Yoshihiro, I., Mori, M., Yamada, K., Oshikawa, Y., Saitoh, H. et al. (2019) Conserved fungal effector suppresses PAMP-triggered immunity by targeting plant immune kinases. *Proceedings of the National Academy of Sciences of the United States of America*, 116, 496–505.

Jones, P., Binns, D., Chang, H., Fraser, M., Li, W., McAnulla, C. et al. (2014) InterProScan 5: genome-scale protein function classification. *Bioinformatics*, 30, 1236–1240.

Jumper, J., Evans, R., Pritzel, A., Green, T., Figurnov, M., Ronneberger, O. et al. (2021) Highly accurate protein structure prediction with AlphaFold. *Nature*, 596, 583–589.

Kanyuka, K. & Rudd, J.J. (2019) Cell surface immune receptors: the guardians of the plant's extracellular spaces. *Current Opinion in Plant Biology*, 50, 1–8.

Karki, S.J., Reilly, A., Zhou, B., Mascarello, M., Burke, J. & Doohan, F. (2018) A small secreted protein from *Zymoseptoria tritici* interacts with a wheat E3 ubiquitin ligase to promote disease. *Journal of Experimental Botany*, 72, 733–746.

Kettles, G.J., Bayon, C., Canning, G., Rudd, J.J. & Kanyuka, K. (2017) Apoplastic recognition of multiple candidate effectors from the wheat pathogen *Zymoseptoria tritici* in the nonhost plant *Nicotiana benthamiana*. *New Phytologist*, 213, 338–350.

Kettles, G.J., Bayon, C., Sparks, C.A., Canning, G., Kanyuka, K. & Rudd, J.J. (2018) Characterization of an antimicrobial and phytotoxic ribonuclease secreted by the fungal wheat pathogen *Zymoseptoria tritici*. *New Phytologist*, 217, 320–331.

Köster, P., DeFalco, T.A. & Zipfel, C. (2022) Ca^{2+} signals in plant immunity. *The EMBO Journal*, 41, e110741.

Lauge, R., Joosten, M.H.A.J., Haanstra, J.P.W., Goodwin, P.H., Lindhout, P. & De Wit, P.J.G.M. (1998) Successful search for a resistance gene in tomato targeted against a virulence factor of a fungal pathogen. *Proceedings of the National Academy of Sciences of the United States of America*, 95, 9014–9018.

Liebrand, T.W.H., van den Burg, H.A. & Joosten, M.H.A.J. (2013) Two for all: receptor-associated kinases SOBIR1 and BAK1. *Trends in Plant Science*, 19, 123–132.

Lu, S. & Faris, J.D. (2019) *Fusarium graminearum* KP4-like proteins possess root growth-inhibiting activity against wheat and potentially contribute to fungal virulence in seedling rot. *Fungal Genetics and Biology*, 123, 1–13.

Marshall, R., Kombrink, A., Motteram, J., Loza-Reyes, E., Lucas, J., Hammond-Kosack, K.E. et al. (2011) Analysis of two *in planta* expressed LysM effector homologs from the fungus *Mycosphaerella graminicola* reveals novel functional properties and varying contributions to virulence on wheat. *Plant Physiology*, 156, 756–769.

M'Barek, S.B., Cordewener, J.H.G., Ghaffary, S.M.T., van der Lee, T.A.J., Liu, Z., Gohari, A.M. et al. (2015) FPLC and liquid-chromatography mass spectrometry identify candidate necrosis-inducing proteins from culture filtrates of the fungal wheat pathogen *Zymoseptoria tritici*. *Fungal Genetics and Biology*, 79, 54–62.

Meile, L., Croll, D., Brunner, P.C., Plissonneau, C., Hartmann, F.E., McDonald, B. et al. (2018) A fungal avirulence factor encoded in a highly plastic genomic region triggers partial resistance to Septoria tritici blotch. *New Phytologist*, 219, 1048–1061.

Mesarich, C.H., Ökmen, B., Rovenich, H., Griffiths, S.A., Wang, C., Jashni, M.K. et al. (2018) Specific hypersensitive response–associated recognition of new apoplastic effectors from *Cladosporium fulvum* in wild tomato. *Molecular Plant–Microbe Interactions*, 31, 145–162.

Noei, F.N., Imami, M., Didaran, F., Ghanbari, M.A., Zamani, E., Ebbrahimi, A. et al. (2022) Stb6 mediates stomatal immunity, photosynthetic functionality, and the antioxidant system during the *Zymoseptoria tritici*–wheat interaction. *Frontiers in Plant Science*, 13, 1004691.

Rocafort, M., Bowen, J.K., Hassing, B., Cox, M.P., McGreal, B., de la Rosa, S. et al. (2022) The *Venturia inaequalis* effector repertoire is dominated by expanded families with predicted structural similarity, but unrelated sequence, to avirulence proteins from other plant-pathogenic fungi. *BMC Biology*, 20, 246.

Rudd, J.J., Kanyuka, K., Hassani-Pak, K., Derbyshire, M., Andongabo, A., Devonshire, J. et al. (2015) Transcriptome and metabolite profiling of the infection cycle of *Zymoseptoria tritici* on wheat reveals a biphasic interaction with plant immunity involving differential pathogen chromosomal contributions and a variation on the hemibiotrophic lifestyle definition. *Plant Physiology*, 167, 1158–1185.

Sánchez-Vallet, A., McDonald, M.C., Solomon, P.S. & McDonald, B.A. (2015) Is *Zymoseptoria tritici* a hemibiotroph? *Fungal Genetics and Biology*, 79, 29–32.

Sánchez-Vallet, A., Tian, H., Rodriguez-Moreno, Valkenburg, D. & Saleema-Batcha, Wara, S. (2020) A secreted LysM effector protects fungal hyphae through chitin-dependent homodimer polymerization. *PLoS Pathogens*, 16, e1008652.

Saur, I.M.L., Bauer, S., Lu, X. & Schulze-Lefert, P. (2019) A cell death assay in barley and wheat protoplasts for identification and validation of matching pathogen AVR effector and plant NLR immune receptors. *Plant Methods*, 15, 118.

Seong, K. & Krasileva, K.V. (2023) Prediction of effector protein structures from fungal phytopathogens enables evolutionary analyses. *Nature Microbiology*, 8, 174–187.

Seybold, H., Demetrowitsch, T.J., Hassani, M.A., Szymczak, S., Reim, E., Haueisen, J. et al. (2020) A fungal pathogen induces systemic susceptibility and systemic shifts in wheat metabolome and microbiome composition. *Nature Communications*, 11, 1910.

Sperschneider, J., Dodds, P.N., Gardiner, D.M., Singh, K.B. & Taylor, J.M. (2018) Improved prediction of fungal effector proteins from secretomes with EffectorP 2.0. *Molecular Plant Pathology*, 19, 2094–2110.

Stamatakis, A. (2006) RAxML-VI-HPC: maximum likelihood-based phylogenetic analyses with thousands of taxa and mixed models. *Bioinformatics*, 22(21), 2688–2690.

Stotz, H.U., Mitrousia, G.K., de Wit, P.J.G.M. & Fitt, B.D.L. (2014) Effector-triggered defence against apoplastic fungal pathogens. *Trends in Plant Science*, 19, 491–500.

Stukenbrock, E.H., Christiansen, F.B., Hansen, T.T., Dutheil, J.Y. & Schierup, M.H. (2012) Fusion of two divergent fungal individuals led to the recent emergence of a unique widespread pathogen species. *Proceedings of the National Academy of Sciences of the United States of America*, 109, 10954–10959.

Tian, H., MacKenzie, C.I., Rodriguez-Moreno, L., Grardy, C.M.V.D.M., Chen, H., Rudd, J.J. et al. (2021) Three LysM effectors of *Zymoseptoria tritici* collectively disarm chitin-triggered plant immunity. *Molecular Plant Pathology*, 22, 683–693.

Torriani, S.F.F., Melichar, J.P.E., Mills, C., Pain, N., Sierotzki, H. & Courbot, M. (2015) *Zymoseptoria tritici*: a major threat to wheat production, integrated approaches to control. *Fungal Genetics and Biology*, 79, 8–12.

van Kempen, M., Kim, S.S., Tumescheit, C., Mirdita, M., Lee, J., Gilchrist, C.L.M. et al. (2024) Fast and accurate protein structure search with Foldseek. *Nature Biotechnology*, 42, 243–246.

Varadi, M., Anyango, S., Deshpande, M., Nair, S., Natassia, C., Yordanova, G. et al. (2022). AlphaFold Protein Structure Database: massively expanding the structural coverage of protein-sequence space with high-accuracy models. *Nucleic Acids Research*, 50(D1), D439–D444.

Wang, C. & Luan, S. (2024) Calcium homeostasis and signaling in plant immunity. *Current Opinion in Plant Biology*, 77, 102485.

Welch, T., Bayon, C., Rudd, J.J., Kanyuka, K. & Kettles, G.J. (2022) Induction of distinct plant cell death programs by secreted proteins from the wheat pathogen *Zymoseptoria tritici*. *Scientific Reports*, 12, 17880.

Wilson, S., Dagvadorj, B., Tam, R., Murphy, L., Schulz-Kroenert, S., Heng, N. et al. (2024) Multiplexed effector screening for recognition by endogenous resistance genes using positive defense reporters in wheat protoplasts. *New Phytologist*, 241, 2621–2636.

Yu, D.S., Outram, M.A., Smith, A., McCombe, C.L., Khambalkar, P.B., Rima, S.A. et al. (2023) The structural repertoire of *Fusarium oxysporum* f. sp. *lycopersici* effectors revealed by experimental and computational studies. *eLife*, 27, RP89280.

Zhang, H., Hu, Z., Lei, C., Zheng, C., Wang, J., Shao, S. et al. (2018) A plant phytosulfokine peptide initiates auxin-dependent immunity through cytosolic Ca^{2+} signaling in tomato. *The Plant Cell*, 30, 652–667.

Zhao, Y., Zheng, X., Tabima, J.F., Zhu, S., Sondreli, K.L., Hundley, H. et al. (2023) Secreted effector proteins of poplar leaf spot and stem canker pathogen *Sphaerulina musiva* manipulate plant immunity and contribute to virulence in diverse ways. *Molecular Plant–Microbe Interactions*, 36, 779–795.

Zhong, Z., Marcel, T.C., Hartmann, F.E., Ma, X., Plissonneau, C., Zala, M. et al. (2017) A small secreted protein in *Zymoseptoria tritici* is responsible for avirulence on wheat cultivars carrying the *Stb6* resistance gene. *New Phytologist*, 214, 619–631.

Ziemann, S., van der Linde, K., Lahrmann, U., Acar, B., Kaschani, F., Colby, T. et al. (2018) An apoplastic peptide activates salicylic acid signalling in maize. *Nature Plants*, 4, 172–180.

SUPPORTING INFORMATION

Additional supporting information can be found online in the Supporting Information section at the end of this article.